ANTIOXIDANTS & REDOX SIGNALING
Volume 14, Number 12, 2011

DOI: 10.1089/ars.2010.3150

ORIGINAL RESEARCH COMMUNICATION

# Connexin43 Hemichannels Contribute to Cadmium-Induced Oxidative Stress and Cell Injury

Xin Fang,[1,2] Tao Huang,[1] Ying Zhu,[1] Qiaojing Yan,[1] Yuan Chi,[1] Jean X. Jiang,[3] Peiyu Wang,[4] Hiroyuki Matsue,[5] Masanori Kitamura,[1] and Jian Yao[1]

## Abstract

We investigated the potential involvement of connexin hemichannels in cadmium ions ($Cd^{2+}$)-elicited cell injury. Transfection of LLC-PK1 cells with a wild-type connexin43 (Cx43) sensitized them to $Cd^{2+}$-elicited cell injury. The cell susceptibility to $Cd^{2+}$ was increased by depletion of glutathione (GSH) with DL-buthionine-[S,R]-sulfoximine, and decreased by N-acetyl-cysteine or glutathione reduced ethyl ester. Fibroblasts derived from Cx43 wild-type (Cx43+/+) and knockout (Cx43-/-) fetal littermates displayed different susceptibility to $Cd^{2+}$. $Cd^{2+}$ induced a higher concentration of reactive oxygen species, a stronger activation c-Jun N-terminal kinase, and significantly more severe cell injury in Cx43+/+ fibroblasts, as compared with Cx43-/- fibroblasts. $Cd^{2+}$ caused a reduction in intracellular GSH, whereas it elevated extracellular GSH. This effect of $Cd^{2+}$ was more dramatic in Cx43+/+ than Cx43-/- fibroblasts. Treatment of Cx43+/+ fibroblasts with $Cd^{2+}$ caused a Cx43 hemichannel-dependent influx of Lucifer Yellow and efflux of ATP. Collectively, our study demonstrates that Cx43 sensitizes cells to $Cd^{2+}$-initiated cytotoxicity, possibly through hemichannel-mediated effects on intracellular oxidative status. *Antioxid. Redox Signal.* 14, 2427–2439.

## Introduction

Cadmium ($Cd^{2+}$) is one of the major metal pollutants. It can be easily accumulated in the vital organs because of its widespread presence and the long half-life (16–33 years). Accumulation of $Cd^{2+}$ causes a variety of pathological situations, including neurodegeneration, dysfunction of liver, lung, and kidney, as well as disorders in blood and vascular systems (13, 15). $Cd^{2+}$ is toxic to multiple cell types. Most of the toxic effects of $Cd^{2+}$ are mediated by oxidative stress (26, 52). $Cd^{2+}$ promotes the formation of oxygen free radicals (12) and decreases the concentration of the important antioxidant glutathione (GSH) (23, 29). Modulation of intracellular redox status or inhibition of the stress-related signal such as c-Jun N-terminal kinase (JNK) has been documented to attenuate and even prevent $Cd^{2+}$-initiated cell injury (37, 40, 52).

Gap junctions are specialized membrane regions composed of aggregates of channels that permit the direct exchange of ions, secondary messengers, and small signaling molecules among neighboring cells. Each gap junction channel is composed of two hemichannels that reside in the plasma membrane of two closely apposed cells. The proteins that form the gap junctions are called connexin (Cx). Up to now, more than 20 different Cx molecules have been identified. Among them, Cx43 has been extensively investigated because of its ubiquitous expression in a variety of cell types.

Intercellular communication via gap junctions is thought to play an important role in regulation of cell functions including cell proliferation, migration, differentiation, and survival. The majority of the biological effects of gap junctions are mediated by the direct transmission of signaling molecules among neighboring cells. Gap junctions also exert biological effects by mechanisms independent of cell-to-cell communication (35, 46, 48).

Gap junctions have been implicated in various pathological situations, including those caused by oxidative stress. Gap junctions, on the one hand, are subjected to the regulation of oxidative stress (1, 3–5). On the other hand, they impact cell responses to oxidative stress-initiated cell injury (2, 19, 32). Depending on the type and extent of injuries, as well as the nature of insults, gap junctions can either attenuate or exacerbate the cell injury (2, 24, 25, 32). At present, little information is available as to how gap junctions influence

[1]Department of Molecular Signaling, University of Yamanashi, Yamanashi, Japan.
[2]School of Basic Medical Sciences, Inner Mongolia Medical College, Hohhot, China.
[3]Department of Biochemistry, University of Texas Health Science Center, San Antonio, Texas.
[4]Department of Social Medicine and Health Education, School of Public Health, Peking University, Beijing, China.
[5]Department of Dermatology, Chiba University School of Medicine, Chiba, Japan.

oxidative stress. Besides intercellular gap junction channels, the nonjunctional Cx hemichannels may participate in the regulation of cell death and survival through the release of the mediators as ATP, NAD(+), or glutamate (9). The open hemichannels have been reported in a variety of pathological situations, including those involving oxidative stress, such as ischemia (32, 41). We therefore asked whether gap junctions and/or hemichannels could contribute to $Cd^{2+}$-initiated oxidative stress and cell injury. Using a cell culture model, we tested this possibility. Here we present our evidence showing that Cx43 affects cell responses to $Cd^{2+}$, possibly due to the hemichannel-mediated efflux of antioxidant GSH. Targeting Cx molecules could be a promising therapeutic strategy for prevention and treatment of oxidative stress-initiated cell injury.

## Materials and Methods

### Reagents

GSH-Glo™ assay kit was purchased from Promega (Madison, WI). Fetal bovine serum, trypsin/EDTA, antibiotics, N-acety-1-cysteine (NAC), 2′, 7′-dichlorofluorescein diacetate (DCF-DA), cadmium chloride ($CdCl_2$), DL-buthionine-[S,R]-sulfoximine (BSO), and glutathione reduced ethyl ester (GSHee), heptanol, lindane, lucifer yellow (LY) and all other chemicals were obtained from Sigma (Tokyo, Japan). Antibodies against the JNK protein were obtained from Cell Signaling Inc (Beverly, MA).

### Cells

Porcine kidney epithelial cell line LLC-PK1 was purchased from American Type Culture Collection (Rockville, MD). Mouse embryonic fibroblasts were derived from the fetal offspring of mating pairs of heterozygous Cx43 knockout mice (B6, 129-Gjal < tm1Kdr + /- mice; Jackson Laboratories, Bar Harbor, ME),using a method described by Ehlich *et al.* with minor modifications (8, 14). Briefly, both mouse forelimbs were taken from fetuses at day 18 of gestation, minced and digested in DMEM/F12 containing 0.1% collagenases for 30 min. Freed cells were collected and cultured in DMEM/F12 medium containing 15% FBS. Cells at passages between 5 and 15 were used for this study. Genotypes of individual mice and established cell lines were analyzed by PCR.

### Formazan assay

The cell viability was assessed by formazan assay using Cell Counting Kit-8 (Dojindo Laboratory, Kumamoto, Japan) as described before (51, 52).

### Western blot analysis

Total cellular protein was extracted by suspending the prewashed cells in SDS lysis buffer (62.5 m*M* Tris-HCl, 2%SDS, 10% glycerol) together with freshly added proteinase inhibitor cocktail (Nacalai Tesque, Kyoto, Japan). Lysates were incubated on ice for 30 min with intermittent mixing and then centrifuged at 12,000 rpm for 10 min at 4°C. Supernatant was recovered and protein concentration was determined using the Micro BCA Protein Assay Kit (Pierce, Rockford, IL).

Western blot was performed by the enhanced chemiluminescence system (14, 52) Briefly, extracted cellular proteins were separated by 10% SDS-polyacrylamide gels and electrotransferred onto polyvinylidine difluoride membranes. After blocking with 3% bovine serum albumin in PBS, the membranes were incubated with anti-phospho-JNK antibody (Cell Signaling, Beverly, MA). After washing, the membranes were probed with horseradish peroxidase-conjugated anti-rabbit IgG (Cell Signaling), and the bands were visualized by the enhanced chemiluminescence system (Amersham Biosciences, Buckinghamshire, UK). The chemiluminescent signal is captured with a Fujifilm luminescent image LAS-1000 analyzer (Fujifilm, Tokyo, Japan) with an exposure time of 3 min and quantified with densitometric software Fujifilm Image Gauge. To confirm equal loading of proteins, the membranes were stripped with 62.5 m*M* Tris-HCl (pH 6.8) containing 2% SDS and 100 m*M* $\beta$-mercaptoethanol for 30 min at 60°C and reprobed for total JNK protein or $\beta$-actin.

### Detection of reactive oxygen species

The generation of reactive oxygen species (ROS) was detected by dichlorofluorescin fluorescence. Cells grown in 96-well plates were loaded with ROS-responsive fluorescent probe DCF-DA for 1 h and then stimulated with $Cd^{2+}$ for 2 h. After that, the immunofluorescence image was visualized using a fluorescent Olympus IX71 inverted microscope (Olympus, Hachioji-shi, Tokyo, Japan). DCF fluorescence intensity was also quantified (excitation = 485, emission = 510 nm) using a fluorescence multiwell plate reader (Bio-Tek Instruments®).

### ATP measurement

ATP was measured using a luciferin/luciferase bioluminescence assay kit (Molecular Probes, Eugene, OR). The intensity of chemiluminescent signal was determined by a luminometer (Gene Light 55; Microtech Nition, Chiba, Japan) as described before (47).

### Calcein-AM/Propidium Iodide Cell-Survival Assay

Cell viability was evaluated by calcein AM/propidium iodide (PI) double staining following the manufacturer's instruction (Dojindo Laboratory, Kumamoto, Japan) (14).

### Cytotoxicity assay

Cytotoxicity was evaluated by the release of lactate dehydrogenase (LDH) using an LDH cytotoxicity detection kit (Takara Bio Inc., Otsu, Shiga, Japan), as described previously (49).

### Transfection of Cells with Cx43

Wild-type Cx43 pEGFP1 and mutant Cx43-pEGFP vectors were kindly gifted by Dr. Oyamada (Department of Pathology, Kyoto Prefectural University of Medicine, Kyoto, Japan). The wild-type Cx43 pEGFP vector was constructed by ligation of the DraI fragment of rat Cx43 cDNA into the SmaI site of the pEGFP-N1 vector (Clontech, Palo Alto, CA). The mutant Cx43-pEGFP, which lacks 24 bases corresponding to amino acid residues 130–137 of rat Cx43 (Δ130–137 Cx43), was designed according to the initial report of Krutovskikh

*et al.* (22, 28). Previous studies demonstrated that cells carrying the mutant vector cannot form active gap junctional intercellular communication (GJIC) (21, 22, 27, 28, 44).

These vectors were transfected into LLC-PK1 cells by using Lipofectamin Plus reagent (Invitrogen, Carlsbad, CA), following the manufacturer's instruction (14, 28). To obtain LLC-PK1 cell clones stably expressing Cx43-EGFP, the selective medium containing 200 $\mu$g/ml G418 was added into the culture and renewed at the 4-day intervals. Clones with high levels of GFP were selected under the fluorescence microscope and used for this study.

### *Transient Transfection of Cells with siRNA*

Fibroblasts were transiently transfected with siRNA specifically targeting Cx43 (Mm_Gja1_2 HP siRNA; Qiagen, Japan) or a negative control siRNA (AllStars Negative Control siRNA) at a final concentration of 20 n*M* using Hyperfect transfection reagent for 48 h. After that, cells were either left untreated or exposed to 30 $\mu M$ $Cd^{2+}$ for additional 24 h. Cell viability was then evaluated by formazan formation. Cellular proteins were used for analysis of Cx43 levels.

### *GSH measurement*

GSH activity was measured by using GSH-Glo™ assay kit (Promega) (52). Briefly, cells at confluent culture in 96-well culture plates were exposed to 30 $\mu M$ $Cd^{2+}$ for 6 h. The supernatants were collected for measurement of extracellular GSH. The remaining cells were used for evaluation of intracellular GSH according to the protocols provided by the manufacturer.

### *Dye uptake assay*

The presence of functional hemichannels was evaluated by LY uptake as described previously (32, 36). Fibroblasts in the normal culture media were exposed to 30 $\mu M$ $Cd^{2+}$ in the presence or absence of Cx channel inhibitor heptanol (3 m*M*) or lindane (100 $\mu M$) for 12 h. After the treatment, cells were exposed to 0.1% LY in the same medium for an additional 5 min. The cells were then rinsed and fixed with 3% paraformaldehyde and photographed.

### *Statistical analysis*

Values are expressed as mean ± S.E. Comparison of two populations was made by Student *t*-test. For multiple comparisons, one-way analysis of variance (ANOVA) followed by Dunett's test was employed. Both analyses were done by using the SigmaStat statistical software (Jandel Scientific, San Rafael, CA). $P < 0.05$ was considered to be a statistically significant difference.

## Results

### *Exogenous expression of Cx43 sensitizes gap junction-deficient LLC-PK1 cells to $Cd^{2+}$-induced cell injury*

Gap junctions influence cell survival in various pathological situations (2, 14, 19, 24, 25, 32). To evaluate the roles of gap junctions in $Cd^{2+}$-elicited cell injury, a previously well-investigated renal epithelial cell line LLC-PK1 was used. Because this cell line did not express Cx43 nor had the functional GJIC (14, 45), we transfected the cells with a wild-type or a communication-free mutant Cx43-EGFP gene (14, 28). Their responses to $Cd^{2+}$ were compared. As shown in Figure 1A,LLC-PK1 cells positively transfected with wild-type Cx43-EGFP showed plaque-like or linear localization of the fusion protein on the plasma membrane between adjacent cells, whereas the cells with mutant Cx43 displayed the fusion protein both in the cytoplasm and on the plasma membrane. This observation is well consistent with the previous report by Oyamada *et al*. (28).

Exposure of these cells to $Cd^{2+}$ caused an obvious loss of cell viability in wild-type Cx43 cells, but not in mutant Cx43 LLC-PK1 or untransfected control cells (Fig. 1B). Time-course analysis also demonstrated a greater loss of cell viability in wild-type Cx43 LLC-PK1 cells (Fig. 1C). Furthermore, $Cd^{2+}$-elicited cell injury in wild-type Cx43 LLC-PK1 cells was preceded by an appearance of round-shaped cells (Fig. 1D). These observations suggest that expression of a functional Cx43 increases the sensitivity of LLC-PK1 cells to $Cd^{2+}$-induced cell toxicity.

In further support of a role of gap junctions, treatment of wild-type Cx43 LLC-PK1 cells with Cx channel inhibitors heptanol (3 m*M*) (39, 43) or lindane (100 $\mu M$) could largely abrogate $Cd^{2+}$-elicited cell injury (Figs. 1E and 1F). Besides the cytotoxic effects, $Cd^{2+}$ also had the ability to stimulate LLC-PK1 cell survival. Treatment of cells with 50 $\mu M$ $Cd^{2+}$ for 3 h significantly enhanced formazan formation (Fig. 1C). Lower concentration of $Cd^{2+}$ also tended to increase cell survival (10 $\mu M$ for 9 h in Fig. 1F), although there were some variations in results among different batches of experiments (Fig. 1B).

### *$Cd^{2+}$-elicited cell injury is mediated by oxidative stress*

Accumulating evidence indicates that $Cd^{2+}$-elicited cell injury involves oxidative stress (12, 29, 37). We, therefore, tested whether the cell injury triggered by $Cd^{2+}$ could be influenced by the major antioxidant GSH. As shown in Figure 2, depleting intracellular GSH by incubation of cells with a specific GSH synthesis inhibitor BSO (2.5 m*M*) exaggerated $Cd^{2+}$-induced cell injury, as indicated by the increased number of the round-shaped and/or shrunken cells, as well as the decreased cell survival. On the other hand, increasing intracellular GSH by supply of cells with a GSH precursor NAC (2.0 m*M*) or a membrane-permeable glutathione reduced ethyl ester (GSHee; 2.0 m*M*) attenuated cell injury (Figs. 2A–2C). These results suggest that oxidative stress underlies the $Cd^{2+}$-elicited cell injury and that intracellular GSH concentration influences cell susceptibility to $Cd^{2+}$.

As a downstream signal of oxidative stress, c-Jun N-terminal kinase (JNK) has been reported to mediate $Cd^{2+}$-initiated cell injury (40, 52). Consistently, we also found that JNK inhibitor SP600125 attenuated the $Cd^{2+}$-elicited cell injury (Supplementary Fig. S1; Supplementary Data are available online at www.liebertonline.com/ars). In this context, the degree of cell response to $Cd^{2+}$ should be associated with altered JNK activation. We therefore examined JNK activation. As shown in Figure 3A, $Cd^{2+}$ induced a similar early activation of JNK in both mutant and wild-type Cx43 LLC-PK1 cells, which peaked at 0.5–1 h and returned to near basal

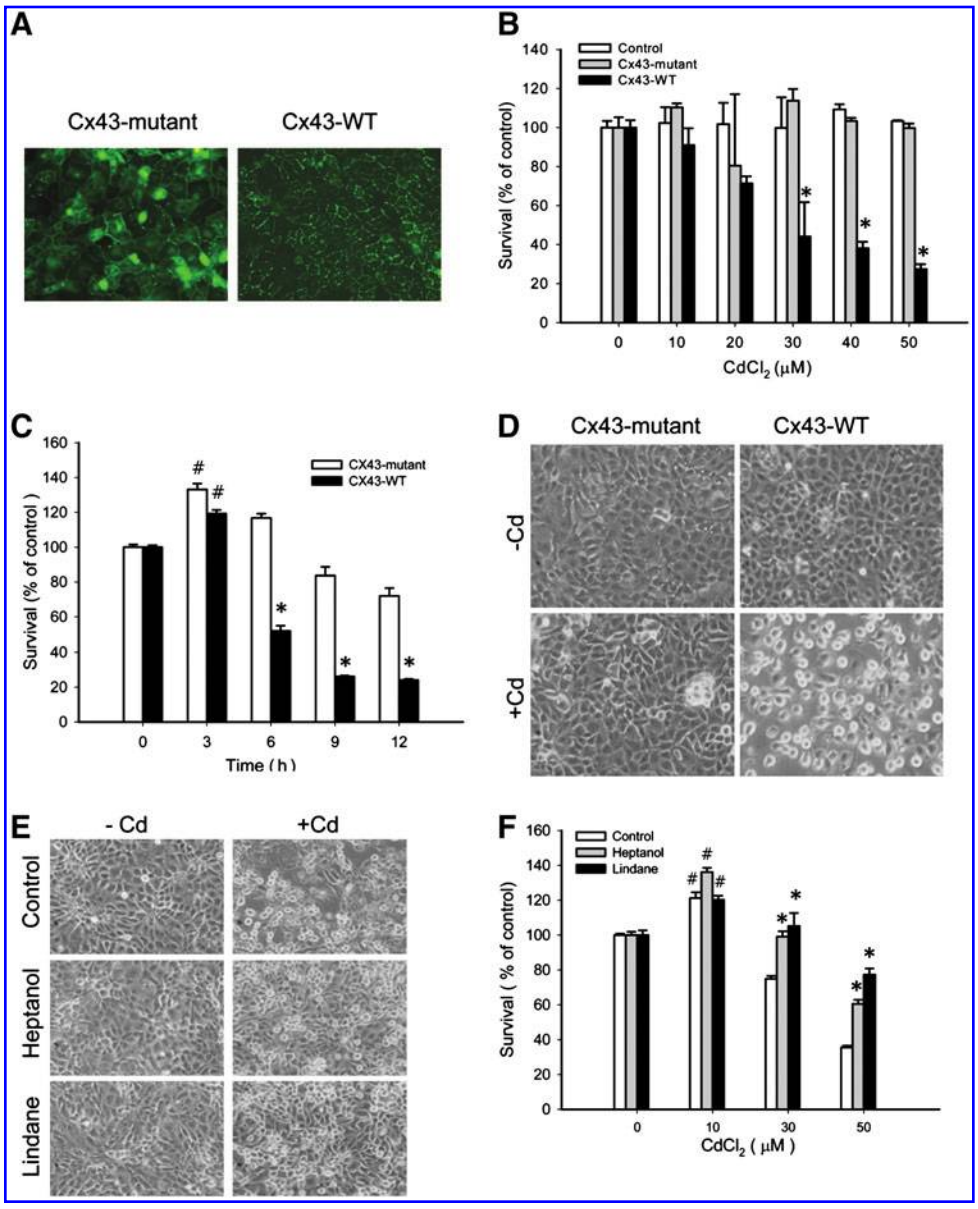


**FIG. 1. Altered cell response to $Cd^{2+}$ after transfection of LLC-PK1 cells with a wild-type Cx43 gene (Cx43-WT). (A)** Cellular localization of Cx43 wild-type and mutant fusion protein in LLC-PK1 cells. LLC-PK1 cells were transfected with a vector encoding mutant or wild-type Cx43 EGFP and clones expressing a high level of fusion protein were selected. The expression and localization of Cx43-EGFP was shown. **(B)** and **(C)** Effects of $Cd^{2+}$ on cell viability. LLC-PK1 cells were treated with various concentrations of $Cd^{2+}$ for 9 h **(B)** or 50 $\mu M$ $Cd^{2+}$ for the indicated times **(C).** Cell viability was measured by formazan assay. The data were expressed as percent of the respective control at zero point (mean ± SE, $n = 4$), $^*p < 0.01$ *vs.* Cx43-mutant LLC-PK1 cells, $\#p < 0.01$ vs. respective zero point control. **(D)** $Cd^{2+}$-elicited cell shape change. LLC-PK1 cells were exposed to 50 $\mu M$ $Cd^{2+}$ (Cd) for 6 h and cell morphology was recorded (X400). **(E)** and **(F)** Prevention of $Cd^{2+}$-induced cell injury by Cx channel inhibitors. **(E)** Effect of Cx channel inhibitors on cell shape. Cx43-WT LLC-PK1 cells were pretreated with or without 3 m$M$ heptanol or 100 $\mu M$ lindane for 30 min before exposing to 50 $\mu M$ $Cd^{2+}$ for an additional 6 h. The cell morphology was recorded. (Magnification, X400). **(F)** Cx channel inhibitors on cell survival. Cx43-WT LLC-PK1 cells were exposed to $Cd^{2+}$ in the presence or absence of 3 m$M$ heptanol or 100 $\mu M$ lindane for 9 h. Cellular viability was determined by formazan assay. The data were expressed as percent of the respective control at zero point (mean ± SE, $n = 6$), $^*p < 0.01$ *vs.* respective $Cd^{2+}$-treated control, $\#p < 0.01$ *vs.* respective zero point control. (To see this illustration in color the reader is referred to the web version of this article at www.liebertonline.com/ars).

levels afterward. However, JNK activation in wild-type Cx43-LLC-PK1 cells rebounded after 6 h. A clear activation of JNK could be observed at 12 h in wild-type Cx43 LLC-PK1 cells, but not in mutant Cx43 cells (Fig. 3A). Concentration-effect analysis revealed that $Cd^{2+}$ induced a much stronger activation of JNK in wild-type Cx43 LLC-PK1 cells than Cx43-mutant cells at the time point of 6 h (Figs. 3B and 3C).

In support of a close link between oxidative stress and JNK activation, modification of intracellular redox status with GSH-regulating agents caused a corresponding change in JNK activation. Depleting the intracellular GSH with BSO enhanced, whereas increasing intracellular GSH with NAC or GSHee decreased JNK activation (Figs. 3D–3F).

Collectively, these observations indicate that oxidative stress plays an important role in $Cd^{2+}$-induced cell injury.

### *Fibroblasts derived from Cx43 wild-type, heterozygous and knockout littermates display different vulnerability to $Cd^{2+}$*

To further establish the role of gap junctions in $Cd^{2+}$-elicited cell injury, we cultured fetal forearm fibroblasts from Cx43 wild-type (Cx43+/+), heterozygous (Cx43+/-) and knockout (Cx43-/-) littermates. In the previous studies, we and others have shown that these cells express different levels of Cx43 and displayed different capacity in GJIC (8, 14, 45).

Incubation of fibroblasts with $Cd^{2+}$ also caused a concentration-dependent loss of cell viability. This is evidenced by the decreased number of calcein AM-stained living cells (Fig. 4A) and the increased number of PI-stained dead cells (Fig. 4B). The extent of cell injury was much more severe

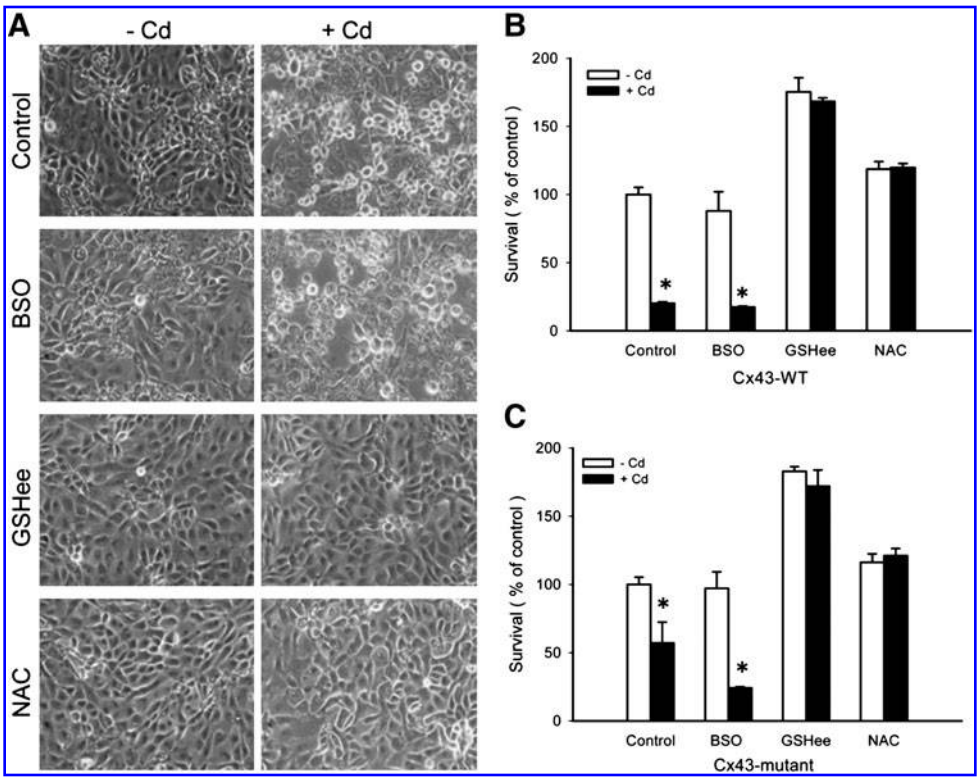


**FIG. 2. Effects of GSH-regulating agents on $Cd^{2+}$-induced cell injury. (A)** GSH-regulating agents on cell shape change. Cx43-WT LLC-PK1 cells were pretreated with 2.5 m*M* BSO for 4 h, 2 m*M* GSHee or 2 m*M* NAC for 1 h, and exposed to 50 $\mu M$ $Cd^{2+}$ for additional 6 h. The cell morphology was photographed (magnification, X 400). **(B)** and **(C)** GSH-regulating agents on cell viability in Cx43-WT **(B)** and Cx43-mutant LLC-PK1 cells **(C).** Cells were exposed to $Cd^{2+}$ in the presence or absence of GSH-regulating agents as described above for 9 h. Cell viability was determined by formazan assay. The data were expressed as percent of untreated blank control (mean ± SE, $n = 4$), $^*p < 0.01$ *vs.* respective control without $Cd^{2+}$ treatment.

in Cx43-positive fibroblasts (Cx43+/+ and Cx43-/-) than Cx43-/- fibroblasts.

The staining results were confirmed by determination of cell viability using the formazan assay. As shown in Figures 4C and 4D, $Cd^{2+}$ elicited a concentration- and time-dependent loss of cell viability in all three types of fibroblasts. The cytotoxic effect of $Cd^{2+}$ was significantly more severe in Cx43-positive fibroblasts than Cx43-/- cells. Interestingly, similar to LLC-PK1 cells, $Cd^{2+}$ at the lower concentrations also promoted formazan formation. Ten micromolar $Cd^{2+}$ caused a significant increase in formazan formation in all three types of fibroblasts, while 20 $\mu M$ $Cd^{2+}$ caused an elevation in Cx43+/- and Cx43-/- cells (Fig. 4C). At present, the mechanisms underlying this effect of $Cd^{2+}$ are still unclear. Because we wanted to focus our study on the roles of Cx43 in cell injury, further investigation on this effect of $Cd^{2+}$ has not been done.

In further support of the involvement of Cx43 in $Cd^{2+}$-initiated cell injury, downregulation of Cx43 in Cx43+/+ fibroblasts with Cx43 siRNA oligos significantly elevated cell resistance to $Cd^{2+}$ (Fig. 4E). The effectiveness of Cx43 siRNA in downregulation of Cx43 protein was confirmed by Western blot analysis. The blot is shown in the inset of Figure 4E.

To assess the role of oxidative stress in the altered cell response to $Cd^{2+}$, we measured ROS concentration in Cx43+/+, Cx43+/-, and Cx43-/- fibroblasts by using a ROS-responsive fluorescence probe, DCF-DA (52). As shown in Figure 5A, under the basal situation, a minimal level of fluorescence signals was detectable among all the fibroblasts tested. However, in the presence of $Cd^{2+}$, the intensity of fluorescence was enhanced. The increment was more pronounced in Cx43+/+ fibroblasts than in Cx43-/- fibroblasts. In a separate experiment, quantification of the DCF fluorescence intensity using a multiplate reader revealed that $Cd^{2+}$ addition significantly increased ROS concentration in Cx43+/+ fibroblasts, but not in Cx43-/- fibroblasts (Supplementary Fig. S2).

Consistent with the different concentrations of ROS, the degree of JNK activation among these fibroblasts was also different. As shown in Figures 5B and 5C, $Cd^{2+}$ triggered a time- and concentration-dependent activation of JNK, which was more pronounced in Cx43+/+ fibroblasts than Cx43-/- cells. There was a significance difference in JNK activation between Cx43+/+ and Cx43-/- fibroblasts at the 6 h point. JNK activation by 30 $\mu M$ $Cd^{2+}$ was 1.00 ± 0.18 in Cx43-/- fibroblasts, whereas it was 2.41 ± 0.25 in Cx43+/+ fibroblasts (mean ± SE; $n = 4$, $P < 0.01$). It appeared that the levels of phosphorylated JNK were closely related to Cx43 levels among these fibroblasts (Figs. 5D and 5E). These observations further indicate that Cx43 contribute to $Cd^{2+}$-elicited oxidative stress and cell injury.

Similar to LLC-PK1 cells, the extent of JNK activation could be modulated by GSH-regulating agents (BSO, NAC, and GSHee) (Figs. 5F and 5G). Furthermore, GSH-regulating agents also altered fibroblast susceptibility to $Cd^{2+}$. As shown in Figures 6A and B, depleting intracellular GSH in Cx43+/+ (Fig. 6A) or Cx43-/- fibroblasts (Fig. 6B) with BSO significantly exaggerated, whereas elevating intracellular GSH with NAC or GSHee completely prevented the cytotoxic effect of $Cd^{2+}$. Of note, GSHee alone significantly stimulated the basal formazan formation in both Cx43+/+ and Cx43-/ fibroblasts ($\#P < 0.01$ *vs.* control).

The effects of GSH-regulating agents on cell viability were associated with an obvious change in intracellular GSH concentrations. As shown in Figure 6C, incubation of Cx43+/+ fibroblasts with 2.5 m*M* BSO caused a time-dependent decrease in GSH concentrations. On the contrary, treatment of cells with 2 m*M* NAC pronouncedly elevated intracellular

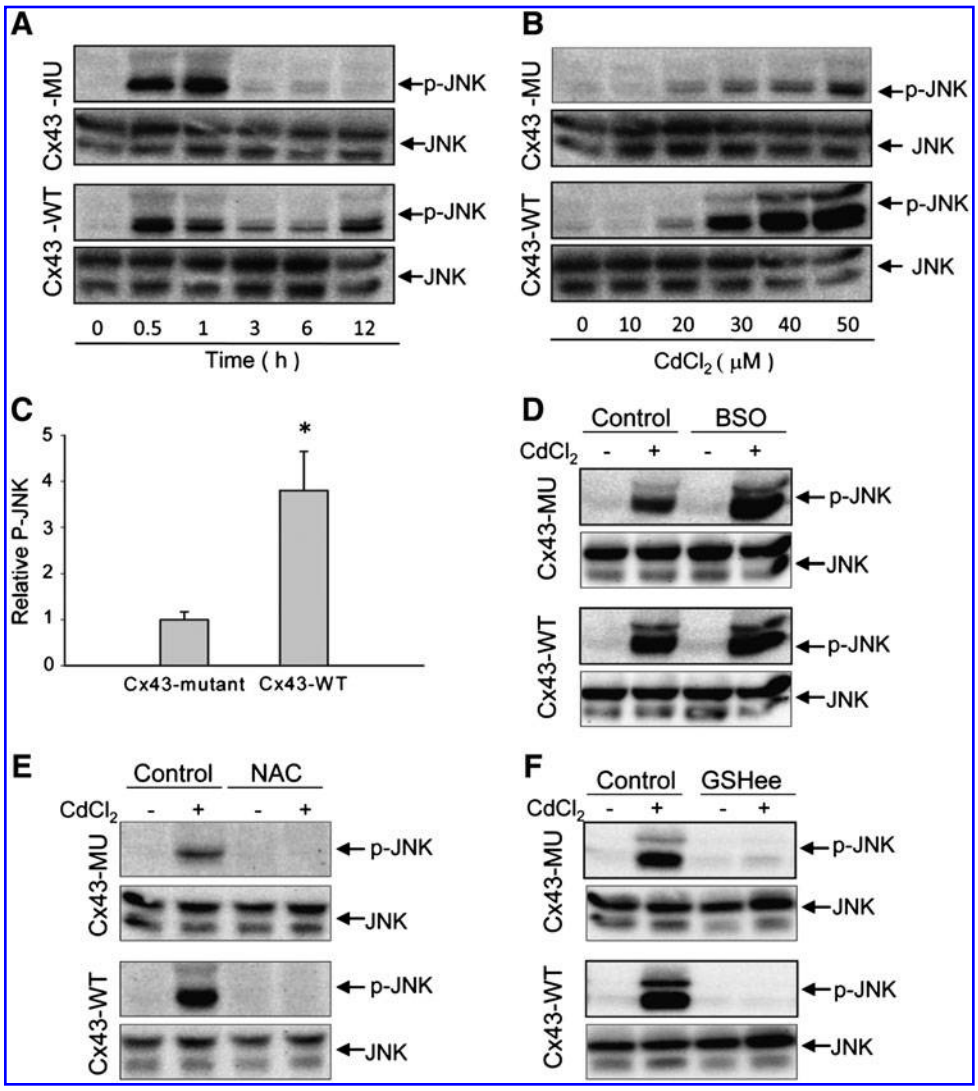


**FIG. 3. $Cd^{2+}$-induced activation of JNK and its modulation by GSH-regulating agents. (A–C)** $Cd^{2+}$-induced JNK activation. LLC-PK1 cells were exposed to 25 $\mu M$ $Cd^{2+}$ for the indicated times **(A)** or various concentrations of $Cd^{2+}$ **(B)** for 6 h. The cellular protein was extracted and subjected to Western blot analysis of phosphorylated (p) JNK. The level of total JNK was taken as loading control. **(C)** The relative intensities of p-JNK signal in Cx43-mutant (Cx43-MU) and Cx43-WT LLC-PK1 cells after exposure to 50 $\mu M$ $Cd^{2+}$ for 6 h. The data are expressed as fold-increase of p-JNK in Cx43-WT LLC-PK1 cells relative to that in Cx43-mutant cells (mean ± SE; $n = 6$, $^*p < 0.05$). **(D)** and **(E)** Modulation of $Cd^{2+}$-induced activation of JNK by GSH-regulating agents. Cx43-WT LLC-PK1 cells were pretreated with 2.5 m$M$ BSO for 4 h **(D)**, 2 m$M$ NAC **(E)**, or 2 m$M$ GSHee for 1 h **(F)**, and then exposed to 50 $\mu M$ $Cd^{2+}$ for additional 6 h. The cellular protein was extracted and subjected to Western blot analysis of JNK.

GSH concentrations. The similar regulatory effects on intracellular GSH and cell susceptibility to $Cd^{2+}$ were also observed in Cx43-/- fibroblasts (Fig. 6D). These results further confirmed the pivotal role of GSH in cell defense against the cytotoxicity of $Cd^{2+}$.

### *$Cd^{2+}$ induces opening of gap junction hemichannels*

The central role of GSH in the regulation of cell response to $Cd^{2+}$ prompted us to ask whether the sensitizing effects of gap junctions were exerted via regulation of intracellular GSH. To test this possibility, we examined the influence of $Cd^{2+}$ on GSH concentrations. As shown in Figures 7A and 7B, incubation of Cx43+/+ fibroblasts with $Cd^{2+}$ caused a time-dependent decrease in intracellular GSH, but an increase in extracellular GSH. In comparison of GSH concentrations between Cx43+/+ and Cx43-/- fibroblasts, we found Cx43+/+ fibroblasts displayed a significantly more pronounced elevation in extracellular GSH concentrations (Fig. 7C), but reduction in intracellular GSH (Fig. 7D), as compared with Cx43-/- cells. This observation suggests that Cx43 may contribute to $Cd^{2+}$-elicited alteration in intra- and extracellular GSH concentrations.

Given opening of Cx hemichannels could lead to extracellular release of small signal molecules such as ATP and GSH (6, 32, 33, 38), we therefore examined the influence of $Cd^{2+}$ on hemichannel opening. As shown in Figure 8A,treatment of Cx43+/+ fibroblasts with 30 $\mu M$ $Cd^{2+}$ for 12 h increased LY uptake, which was largely prevented by Cx channel inhibitors heptanol and lindane. The increase in LY uptake was also observed in Cx43+/+ fibroblasts after 6 h treatment with 50 $\mu M$ $Cd^{2+}$ (Fig. 8B). In accordance with hemichannel opening, $Cd^{2+}$ triggered a more pronounced release of ATP in Cx43-positive fibroblasts than Cx43-negative fibroblasts (Fig. 8C). Of note, $Cd^{2+}$ under the above experimental conditions (30 $\mu M$ $Cd^{2+}$ for 12 h or 50 $\mu M$ for 6 h) did not induce an increase in LDH release (Figs. 8D and 8E).

## Discussion

In this study, we demonstrated, for the first time, that gap junction hemichannels affect cell susceptibility to $Cd^{2+}$. This conclusion is supported by the observations that the cells expressing Cx43 were more sensitive to $Cd^{2+}$ and that downregulation of Cx43 with siRNA or inhibition of Cx43 function with channel inhibitors could significantly enhance

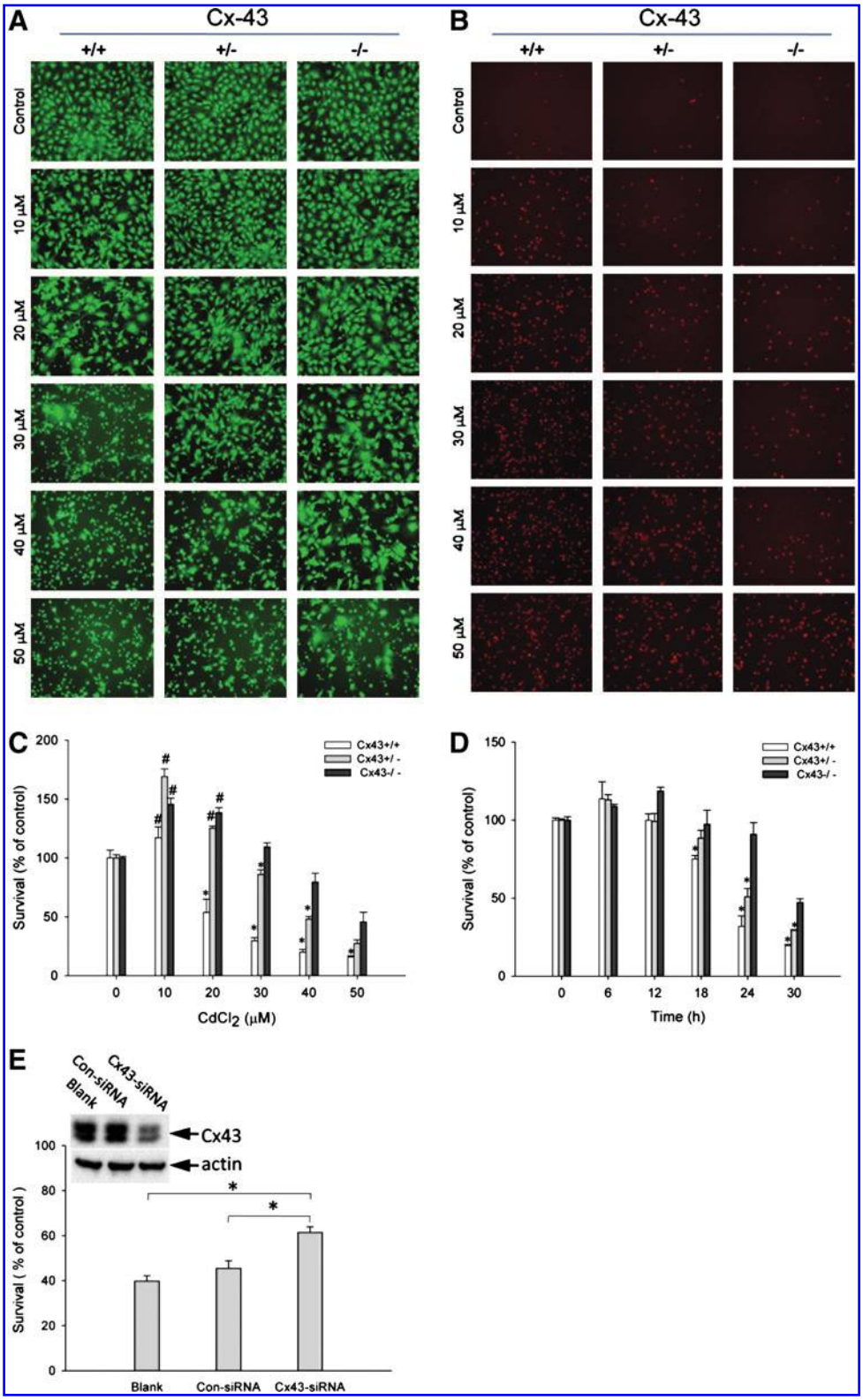


**FIG. 4. Responses of different types of fibroblasts to $Cd^{2+}$-elicited cell injury and its influence by Cx43 siRNA. (A–D)** Cd2+-elicited cell injury in different types of fibroblasts. **(A–C)** Fibroblasts expressing different amounts of Cx43 were exposed to the indicated concentrations of $Cd^{2+}$ for 24 h. The living (**A**) and dead cells (**B**) were identified by calcein AM/PI staining. **(C)** and **(D)** Concentration and time-course effect of $Cd^{2+}$ on cell viability. Fibroblasts were exposed to the indicated concentrations of $Cd^{2+}$ for 24 h **(C)** or 30 $\mu M$ $Cd^{2+}$ for the indicated time **(D).** The cell viability was evaluated by formazan assay. The data are expressed as percent of control at zero point (mean ± SE, $n = 4$), $^*p < 0.01$ *vs.* Cx43-/- fibroblasts, $\#p < 0.05$ *vs.* respective zero point control. **(E)** Downregulation of Cx43 on cell response to $Cd^{2+}$. Cx43+/+ fibroblasts were treated with Cx43 siRNA or control siRNA (Con-siRNA) for 48 h. Cellular proteins were extracted and subjected to Western blot analysis of Cx43. Equal loading of protein was verified by reprobing the blot with anti-$\beta$-actin antibody. Note the obvious reduced level of Cx43 protein in Cx43 siRNA-treated cells (*inset*). The transfected fibroblasts were also examined for cell viability after incubation with 30 $\mu M$ $Cd^{2+}$ for 24 h. Data are expressed as percentage of living cells against the respective untreated control. $^*p < 0.01$ *vs.* siRNA and blank control. (To see this illustration in color the reader is referred to the web version of this article at www.liebertonline.com/ars).

cell resistance to $Cd^{2+}$. Our results also indicate that the effect of Cx43 was correlated with their effects on the intracellular oxidative status. Consistent with the previous reports (26, 52), $Cd^{2+}$-elicited cell injury in LLC-PK1 and fibroblasts was mediated by oxidative stress. This is well evidenced by the increased concentration of ROS, decreased concentration of GSH, activation of JNK, and abrogation of cell injury by GSH (18, 37). Therefore, the different oxidative status among Cx43-positive and -negative cells, as revealed by the different levels of ROS, GSH, and JNK activation, should underlie the varied

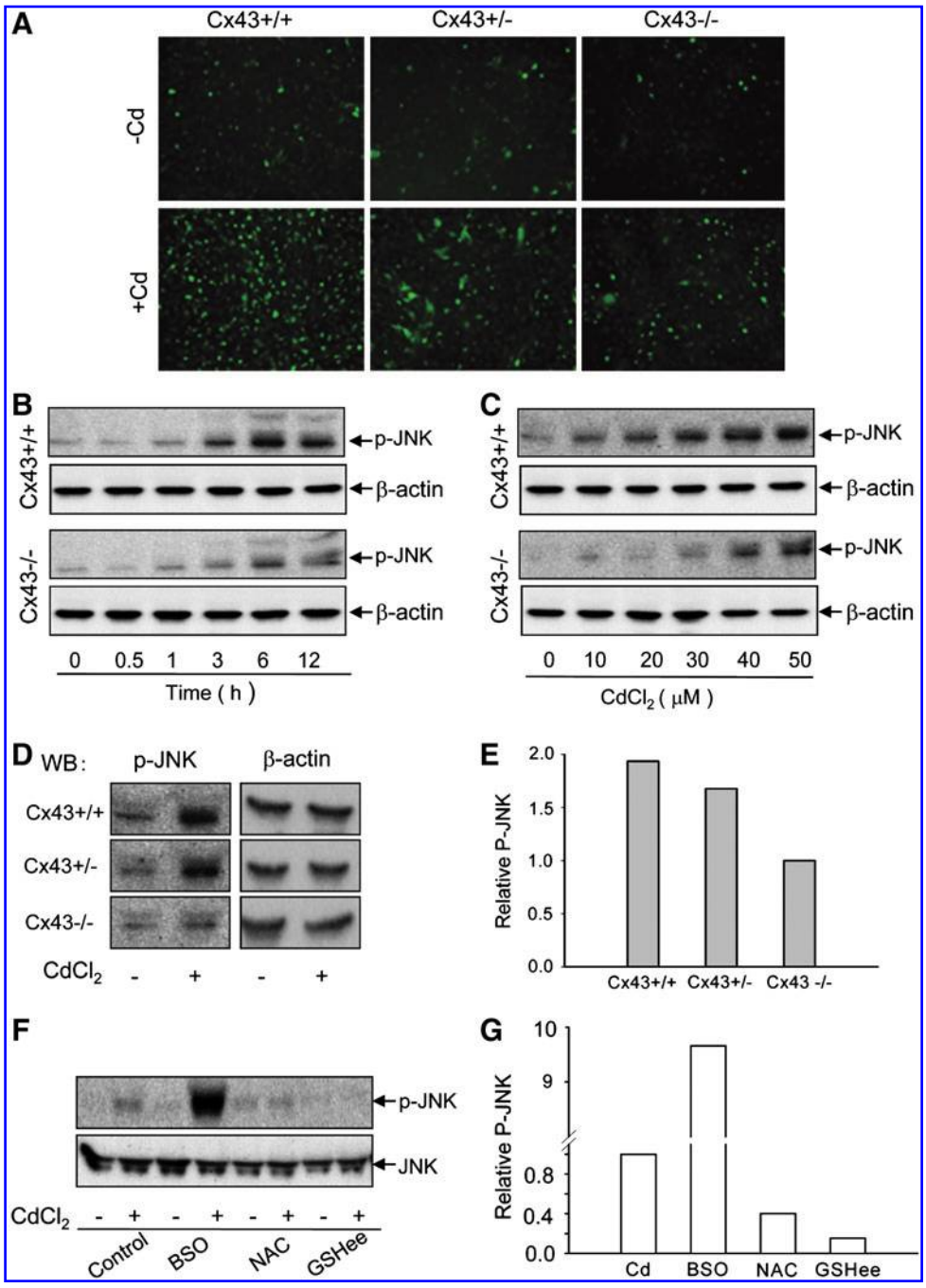


**FIG. 5. $Cd^{2+}$-initiated oxidative stress in Cx43+/+, +/-, and -/- fibroblasts. (A)** Effect of $Cd^{2+}$ on ROS formation. Fibroblasts were loaded with 10 $\mu M$ DCF-DA for 1 h. Cells were stimulated with 30 $\mu M$ $Cd^{2+}$ (Cd) for 2 h and subjected to fluorescent microscopy. (Magnification, X 200). **(B–D)** $Cd^{2+}$-induced JNK activation. Fibroblasts were exposed to 30 $\mu M$ $Cd^{2+}$ for the indicated times **(B)** or various concentrations of $Cd^{2+}$ **(C)** for 6 h. **(D)** JNK activation in different types of fibroblasts. Fibroblasts were exposed to 30 $\mu M$ $Cd^{2+}$ for 6 h. The cellular protein was extracted and subjected to Western blot analysis of p-JNK. Equal loading of protein per lane was verified by probing the blot with an anti-$\beta$-actin antibody. **(E)** The densitometric intensity of p-JNK signal in **B**. The data are expressed as fold-induction of p-JNK relative to that in Cx43-/- fibroblasts. **(F)** Influence of GSH-regulating agents on $Cd^{2+}$-elicited JNK activation. Fibroblasts were pretreated with 2.5 m$M$ BSO for 4 h, 2 m$M$ GSHee or 2 m$M$ NAC for 1 h, and then exposed to 30 $\mu M$ $Cd^{2+}$ for additional 6 h. The cellular protein was extracted and subjected to Western blot analysis of p-JNK. The equal protein loading was confirmed by reprobing the blot with an anti-JNK antibody. **(G)** The densitometric intensity of $Cd^{2+}$-elicited p-JNK signal in **D**. The data are expressed as fold-increase relative to the level of p-JNK in $Cd^{2+}$-treated control cells. (To see this illustration in color the reader is referred to the web version of this article at www.liebertonline.com/ars).

cell responses to $Cd^{2+}$. The question arises as to how Cx43 affected $Cd^{2+}$-initiated oxidative stress and subsequent cell injury. Gap junctions exert multiple pathophysiological functions through communication-dependent and/or -independent mechanism (35, 46, 48). In this study, the cell susceptibility to $Cd^{2+}$ was enhanced by expression of wild-type Cx43 in LLC-PK1 cells, but not a communication-free mutant Cx43 (14, 21, 22, 27, 28, 44), indicating an involvement of functional Cx43. Because $Cd^{2+}$ caused cell shape change before the occurrence of cell injury (a phenomenon that has been observed in multiple cell types and considered to be a result of $Cd^{2+}$-elicited damage of tight junction; 29–31), Cx43-channels in these poorly contacting cells were likely to exist as hemichannels. Indeed, the influx of LY and efflux of ATP was observed in $Cd^{2+}$-treated Cx43-positive cells, supporting the existence of functional Cx hemichannels. As for molecules responsible for the hemichannel-mediated effects on oxidative stress, GSH could be the likely candidate. GSH has been documented to be depleted in $Cd^{2+}$-treated cells (23). As a major oxygen radical scavenger, GSH provides the first line of defense against $Cd^{2+}$-elicited oxidative stress and cell injury (20). Consistently, we also observed that JNK activation and $Cd^{2+}$ toxicity could be up- and downregulated by modulation of intracellular GSH concentrations. Besides the results from the direct measurement of GSH, several observations also suggested an existence of an additional loss of GSH in $Cd^{2+}$-

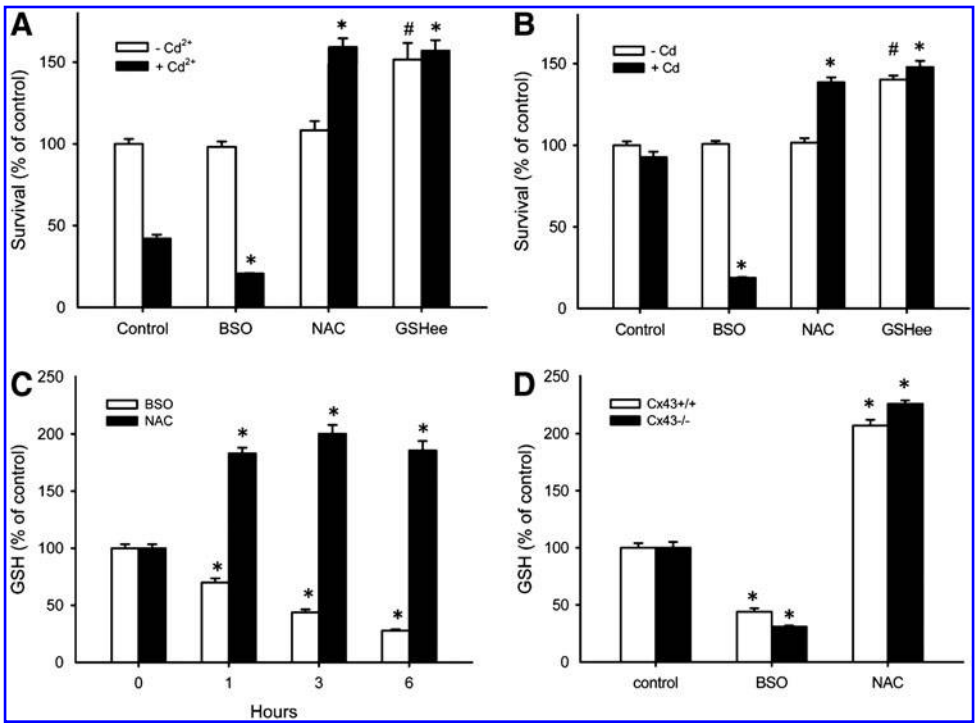


**FIG. 6. Effects of GSH-regulating agents on $Cd^{2+}$-induced cell injury and intracellular GSH concentration. (A, B)** Influence of GSH-modulating agents on $Cd^{2+}$-elicited cell injury in Cx43+/+ **(A)** and Cx43-/- fibroblasts **(B).** Fibroblasts were pretreated with 2.5 m*M* BSO for 4 h, 2 m*M* GSHee or 2 m*M* NAC for 1 h and exposed to 30 $\mu M$ $Cd^{2+}$ for additional 24 h. Cell viability was determined by formazan assay. The data were expressed as percent of untreated blank control (mean ± SE, $n = 4$), $^*p < 0.01$ *vs.* $Cd^{2+}$ control, $\#p < 0.01$ *vs* untreated blank control. **(C)** Time-course effects of GSH-modulating agents on intracellular GSH concentrations in Cx43+/+ fibroblasts. **(D)** Comparison of the effects of GSH-modulating agents on intracellular GSH between Cx43+/+ and Cx43-/- fibroblast. Fibroblasts were exposed to 2.5 m*M* BSO or 2 m*M* NAC for the indicated time period **(C)** or 3 h **(D).** GSH concentrations were measured as described in Methods. The data are expressed as relative change against the untreated control (mean ± SE, $n = 6$). $^*p < 0.01$ *vs.* the respective blank control.

treated Cx43-positive cells. First, the GSH-depleting agent BSO was less effective in potentiation of $Cd^{2+}$-triggered JNK activation and cytotoxicity in wild-type Cx43 LLC-PK1 cells. Second, JNK activation rebounded after 6 h treatment of $Cd^{2+}$, which may reflect a severe deficiency of antioxidant GSH at this time point. Intriguingly, it was well coincident with the time of hemichannel opening. Therefore, it can be assumed that the loss of GSH through Cx43 hemichannels could behind the increased cell vulnerability to $Cd^{2+}$.

The increased cell susceptibility to $Cd^{2+}$ could also result from an elevation in the uptake and retention of $Cd^{2+}$, and/or a decrease in the elimination of the $Cd^{2+}$. At present, the

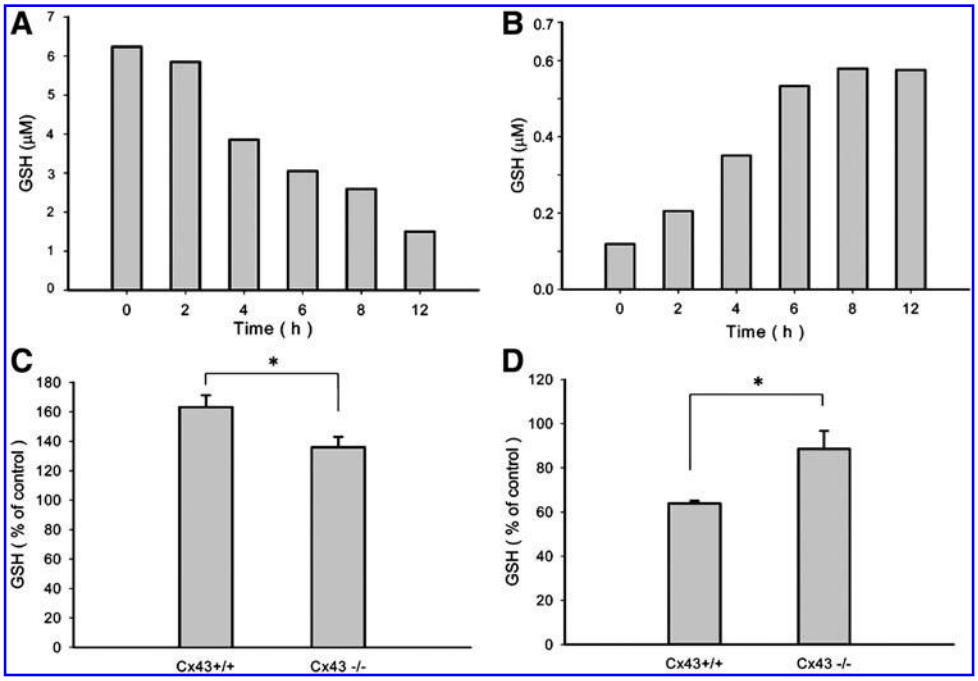


**FIG. 7. Effects of $Cd^{2+}$ on intra- and extracellular GSH concentrations. (A, B)** $Cd^{2+}$ on intra- and extracellular GSH concentrations. Cx43+/+ fibroblasts were exposed to 30 $\mu M$ $Cd^{2+}$ for the indicated times. GSH concentrations in cellular lysates **(A)** and culture supernatants **(B)** were measured as described in Methods. **(C, D)** Change in extra- **(C)** and intracellular **(D)** GSH concentrations between Cx43+/+ and Cx43-/- cells after $Cd^{2+}$ addition. Cells were exposed to 30 $\mu M$ $Cd^{2+}$ for 6 h. GSH was measured as described above. The data are expressed as relative change against the untreated control (mean ± SE, $n = 4$), $^*p < 0.01$.

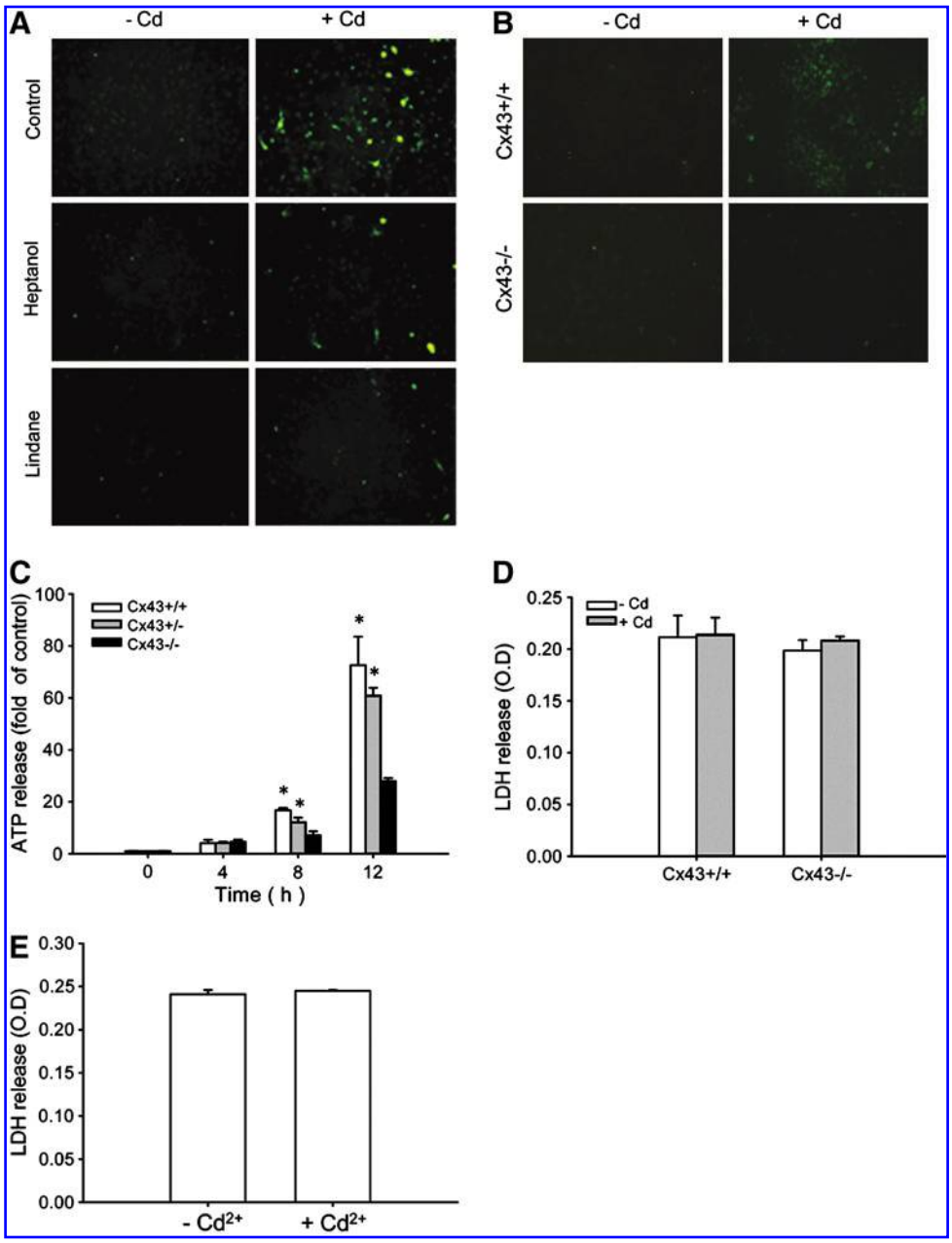


**FIG. 8. Induction of hemichannel opening by $Cd^{2+}$.** **(A)** LY uptake in Cx43+/+ fibroblasts. Cx43+/+ fibroblasts were treated with 30 $\mu M$ $Cd^{2+}$ (Cd) in the presence or absence of Cx channel inhibitors 3 m$M$ heptanol and 100 $\mu M$ lindane for 12 h, and then exposed to 0.1% LY for uptake assay. The immunofluorescent signals were photographed (magnification, X200). **(B)** LY uptake in Cx43+/+ and Cx43-/- fibroblasts. Cx43+/+ fibroblasts were treated with 50 $\mu M$ $Cd^{2+}$ for 6 h and then exposed to 0.1% LY for uptake assay. The immunofluorescent signals were photographed **(B). (C)** $Cd^{2+}$-induced ATP release in fibroblasts expressing different levels of Cx43. Cells were exposed to 30 $\mu M$ $Cd^{2+}$ for 4 h, 8 h, and 12 h, respectively. ATP concentration in culture medium was measured. The data are expressed as the fold induction against zero point (mean ± SE, $n = 4$). *$p < 0.01$ *vs.* Cx43-/- cells. **(D, E)** The effects of $Cd^{2+}$ on LDH release. **(D)** Cx43+/+ and Cx43-/- fibroblasts were treated with 50 $\mu M$ $Cd^{2+}$ for 6 h. **(E)** Cx43+/+ fibroblasts were treated with 30 $\mu M$ $Cd^{2+}$ for 12 h. LDH activity in culture medium was measured. The data are expressed as optical density (OD) values (mean ± SE, $n = 4$). (To see this illustration in color the reader is referred to the web version of this article at www.liebertonline.com/ars).

information on these aspects is still limited. One recent publication showed that hemichannel can promote toxicity of cigarette smoke extract through facilitating the direct entry of toxic molecules (32). The similar scenario may occur in this study. More detailed analysis is required to have a clear conclusion.

The molecular events leading to hemichannel opening are presently unclear. Hemichannel can be opened by membrane depolarization, mechanical stimulation, metabolic stress, reduction in extracellular calcium, and an increase of cytoplasmic calcium (6, 7, 9, 36, 38, 43, 50, 53). In our preliminary study, we noticed that alleviation of oxidative stress with GSH-elevating agents or blockade of JNK activation with SP600125 could largely prevent $Cd^{2+}$-elicited release of ATP (Supplementary Fig. S3),indicating a possible causative role of oxidative stress in hemichannel opening. In line with this notion, a previous report has described that oxidative stress opens gap junction hemichannel via depolarization of the cell membrane (32). In addition, metabolic inhibition-elicited hemichannel opening has been shown to be related to oxidant stress and can be reduced by elevated intracellular GSH concentration (34). In this context, the initial depletion of intracellular GSH concentration by $Cd^{2+}$ could play a critical role in hemichannel opening.

In this study, we reconfirmed the central role of GSH in protection of cells against oxidative stress. $Cd^{2+}$-induced JNK activation and subsequent cell injury could be completely blocked by GSH-elevating agents. As discussed above, depletion of GSH by $Cd^{2+}$ through induction of ROS production might participate in the activation of Cx43 hemichannels, resulting in a further loss of GSH and 'a vicious cycle' between decreased GSH and hemichannel opening. Interestingly, GSH has also been documented to mediate the inhibitory effect of $H_2O_2$ on GJIC. The depletion

of intracellular GSH with BSO completely abolished the inhibitory effect of $H_2O_2$ on GJIC (42). Thus, oxidative stress, gap junctions, and Cx hemichannels could be interlinked by GSH as an integral component of cellular responses to various oxidants. This concept needs to be tested in the future studies.

Of note, several previous studies have demonstrated that $Cd^{2+}$ was able to suppress Cx expression and inhibit GJIC (11, 16, 17). There is also a report documenting that $Cd^{2+}$ exerted different effects on gap junctions, depending on cells, isoforms of Cx tested, as well as time of $Cd^{2+}$ stimulation. In that report, short-term incubation with $Cd^{2+}$ promoted Cx43 phosphorylation and decreased Cx32 expression in normal Balb/3T3 A31 cells, whereas long-term treatment promoted expression of Cx43 and Cx32 in the transformed cells (10). We also examined the influence of $Cd^{2+}$ on Cx43 protein levels and GJIC in fibroblasts. Our results indicated that the levels of Cx43 tended to increase after exposure of Cx43+/+ fibroblasts to high concentrations of $Cd^{2+}$, or after long periods of $Cd^{2+}$ treatment, whereas the function of gap junctions was not greatly altered by $Cd^{2+}$ within 4 h period (Supplementary Fig. S4). At presently, the reasons for the different effects in different cell types and the possible links between the altered Cx43 and hemichannel opening remain to be clarified.

Collectively, our studies characterized Cx43 hemichannel as a presently unrecognized factor affecting cell responses to $Cd^{2+}$. Incubation of cells with $Cd^{2+}$ caused oxidative stress and opening of Cx hemichannels. The efflux of the major antioxidant GSH via the channels will weaken the antioxidative defense, thus sensitizing cell to oxidative stress-induced cell injury. Our findings may have important clinical implications. Beside $Cd^{2+}$, oxidative stress is induced by many insults and has been implicated in a variety of pathological situations. Implication of Cx43 hemichannels in oxidative stress suggests that hemichannel opening could be an important pathogenic factor in these situations. Regulation of hemichannel opening could be a novel approach to prevent and alleviate the stress-associated cell injury.

## Acknowledgments

This work was supported by Grants-in-Aid for Scientific Research from the Ministry of Education, Culture, Sports, Science and Technology, Japan (17659255 and 20590953 to JY; B21390324 to HM), grants from Takeda Science Foundation, Japan–China Medical Association as well as Strategic Project Grant from University of Yamanashi and grants from National Institute of Health (AR 46798 to JXJ) and Welch Foundation (AQ-1507 to JXJ). The authors wish to thank Dr. Kazunori Nakamoto in the Center for Life Science Research of Yamanashi University for his helpful discussion and advice on statistical analyses.

## Author Disclosure Statement

No competing financial interests exist.

## References

1. Aleo MF, Morandini F, Bettoni F, Tanganelli S, Vezzola A, Giuliani R, Steimberg N, Apostoli P, and Mazzoleni G. Antioxidant potential and gap junction-mediated intercellular communication as early biological markers of mercuric chloride toxicity in the MDCK cell line. *Toxicol In Vitro* 16: 457–465, 2002.
2. Azzam EI, de Toledo SM, and Little JB. Direct evidence for the participation of gap junction-mediated intercellular communication in the transmission of damage signals from alpha -particle irradiated to nonirradiated cells. *Proc Natl Acad Sci USA* 98: 473–478, 2001.
3. Azzam EI, de Toledo SM, and Little JB. Oxidative metabolism, gap junctions and the ionizing radiation-induced bystander effect. *Oncogene* 22: 7050–7057, 2003.
4. Bellei B, Mastrofrancesco A, Briganti S, Aspite N, Ale–Agha N, Sies H, and Picardo M. Ultraviolet A induced modulation of gap junctional intercellular communication by P38 MAPK activation in human keratinocytes. *Exp Dermatol* 17: 115–124, 2008.
5. Berthoud VM and Beyer EC. Oxidative stress, lens gap junctions, and cataracts. *Antioxid Redox Signal* 11: 339–353, 2009.
6. Bruzzone S, Guida L, Zocchi E, Franco L, and De Flora A. Connexin 43 hemi channels mediate $Ca^{2+}$-regulated transmembrane NAD+ fluxes in intact cells. *FASEB J* 15: 10–12, 2001.
7. Contreras JE, Saez JC, Bukauskas FF, and Bennett MV. Gating and regulation of connexin 43 (Cx43) hemichannels. *Proc Natl Acad Sci USA* 100: 11388-11393, 2003.
8. Ehrlich HP, Gabbiani G, and Meda P. Cell coupling modulates the contraction of fibroblast-populated collagen lattices. *J Cell Physiol* 184: 86–92, 2000.
9. Evans WH, De Vuyst E, and Leybaert L. The gap junction cellular internet: Connexin hemichannels enter the signalling limelight. *Biochem J* 397: 1–14, 2006.
10. Fang MZ, Mar WC, and Cho MH. Cadmium-induced alterations of connexin expression in the promotion stage of *in vitro* two-stage transformation. *Toxicology* 161: 117–127, 2001.
11. Fukumoto M, Kujiraoka T, Hara M, Shibasaki T, Hosoya T, and Yoshida M. Effect of cadmium on gap junctional intercellular communication in primary cultures of rat renal proximal tubular cells. *Life Sci* 69: 247–254, 2001.
12. Gennari A, Cortese E, Boveri M, Casado J, and Prieto P. Sensitive endpoints for evaluating cadmium-induced acute toxicity in LLC-PK1 cells. *Toxicology* 183: 211–220, 2003.
13. Henson MC and Chedrese PJ. Endocrine disruption by cadmium, a common environmental toxicant with paradoxical effects on reproduction. *Exp Biol Med (Maywood)* 229: 383–392, 2004.
14. Huang T, Zhu Y, Fang X, Chi Y, Kitamura M, and Yao J. Gap junctions sensitize cancer cells to proteasome inhibitor MG132-induced apoptosis. *Cancer Sci* 101: 713–721, 2010.
15. Jarup L and Akesson A. Current status of cadmium as an environmental health problem. *Toxicol Appl Pharmacol* 238: 201–208, 2009.
16. Jeon SH, Cho MH, and Cho JH. Effects of cadmium on gap junctional intercellular communication in WB-F344 rat liver epithelial cells. *Hum Exp Toxicol* 20: 577–583, 2001.
17. Jeong SH, Habeebu SS, and Klaassen CD. Cadmium decreases gap junctional intercellular communication in mouse liver. *Toxicol Sci* 57: 156–166, 2000.
18. Jimi S, Uchiyama M, Takaki A, Suzumiya J, and Hara S. Mechanisms of cell death induced by cadmium and arsenic. *Ann NY Acad Sci* 1011: 325–331, 2004.
19. Johnson LN and Koval M. Cross-talk between pulmonary injury, oxidant stress, and gap junctional communication. *Antioxid Redox Signal* 11: 355–367, 2009.

20. Kim SC, Cho MK, and Kim SG. Cadmium-induced non-apoptotic cell death mediated by oxidative stress under the condition of sulfhydryl deficiency. *Toxicol Lett* 144: 325–336, 2003.
21. Kizana E, Chang CY, Cingolani E, Ramirez–Correa GA, Sekar RB, Abraham MR, Ginn SL, Tung L, Alexander IE, and Marban E. Gene transfer of connexin43 mutants attenuates coupling in cardiomyocytes: Novel basis for modulation of cardiac conduction by gene therapy. *Circ Res* 100: 1597–1604, 2007.
22. Krutovskikh VA, Yamasaki H, Tsuda H, and Asamoto M. Inhibition of intrinsic gap-junction intercellular communication and enhancement of tumorigenicity of the rat bladder carcinoma cell line BC31 by a dominant-negative connexin 43 mutant. *Mol Carcinog* 23: 254–261, 1998.
23. Lawal AO and Ellis E. Differential sensitivity and responsiveness of three human cell lines HepG2, 1321N1 and HEK 293 to cadmium. *J Toxicol Sci* 35: 465–478, 2010.
24. Lin JH, Weigel H, Cotrina ML, Liu S, Bueno E, Hansen AJ, Hansen TW, Goldman S, and Nedergaard M. Gap-junction-mediated propagation and amplification of cell injury. *Nat Neurosci* 1: 494–500, 1998.
25. Lin JH, Yang J, Liu S, Takano T, Wang X, Gao Q, Willecke K, and Nedergaard M. Connexin mediates gap junction-independent resistance to cellular injury. *J Neurosci* 23: 430–441, 2003.
26. Liu J, Qu W, and Kadiiska MB. Role of oxidative stress in cadmium toxicity and carcinogenesis. *Toxicol Appl Pharmacol* 238: 209–214, 2009.
27. Nakagami T, Tanaka H, Dai P, Lin SF, Tanabe T, Mani H, Fujiwara K, Matsubara H, and Takamatsu T. Generation of reentrant arrhythmias by dominant-negative inhibition of connexin43 in rat cultured myocyte monolayers. *Cardiovasc Res* 79: 70–79, 2008.
28. Oyamada Y, Zhou W, Oyamada H, Takamatsu T, and Oyamada M. Dominant-negative connexin43-EGFP inhibits calcium-transient synchronization of primary neonatal rat cardiomyocytes. *Exp Cell Res* 273: 85–94, 2002.
29. Prozialeck WC and Lamar PC. Effects of glutathione depletion on the cytotoxic actions of cadmium in LLC-PK1 cells. *Toxicol Appl Pharmacol* 134: 285–295, 1995.
30. Prozialeck WC and Lamar PC. Cadmium (Cd2+) disrupts E-cadherin-dependent cell-cell junctions in MDCK cells. *In Vitro Cell Dev Biol Anim* 33: 516–526, 1997.
31. Prozialeck WC, Lamar PC, and Lynch SM. Cadmium alters the localization of N-cadherin, E-cadherin, and beta-catenin in the proximal tubule epithelium. *Toxicol Appl Pharmacol* 189: 180–195, 2003.
32. Ramachandran S, Xie LH, John SA, Subramaniam S, and Lal R. A novel role for connexin hemichannel in oxidative stress and smoking-induced cell injury. *PLoS One* 2: e712, 2007.
33. Rana S and Dringen R. Gap junction hemichannel-mediated release of glutathione from cultured rat astrocytes. *Neurosci Lett* 415: 45–48, 2007.
34. Retamal MA, Cortes CJ, Reuss L, Bennett MV, and Saez JC. S-nitrosylation and permeation through connexin 43 hemichannels in astrocytes: induction by oxidant stress and reversal by reducing agents. *Proc Natl Acad Sci USA* 103: 4475–4480, 2006.
35. Saez JC, Berthoud VM, Branes MC, Martinez AD, and Beyer EC. Plasma membrane channels formed by connexins: Their regulation and functions. *Physiol Rev* 83: 1359–1400, 2003.
36. Siller–Jackson AJ, Burra S, Gu S, Xia X, Bonewald LF, Sprague E, and Jiang JX. Adaptation of connexin 43-hemichannel prostaglandin release to mechanical loading. *J Biol Chem* 283: 26374–26382, 2008.
37. Son MH, Kang KW, Lee CH, and Kim SG. Potentiation of cadmium-induced cytotoxicity by sulfur amino acid deprivation through activation of extracellular signal-regulated kinase1/2 (ERK1/2) in conjunction with p38 kinase or c-jun N-terminal kinase (JNK). Complete inhibition of the potentiated toxicity by U0126 an ERK1/2 and p38 kinase inhibitor. *Biochem Pharmacol* 62: 1379–1390, 2001.
38. Stout CE, Costantin JL, Naus CC, and Charles AC. Intercellular calcium signaling in astrocytes via ATP release through connexin hemichannels. *J Biol Chem* 277: 10482–10488, 2002.
39. Takens–Kwak BR, Jongsma HJ, Rook MB, and Van Ginneken AC. Mechanism of heptanol-induced uncoupling of cardiac gap junctions: A perforated patch-clamp study. *Am J Physiol* 262: C1531–1538, 1992.
40. Thevenod F, Friedmann JM, Katsen AD, and Hauser IA. Up-regulation of multidrug resistance P-glycoprotein via nuclear factor-kappaB activation protects kidney proximal tubule cells from cadmium- and reactive oxygen species-induced apoptosis. *J Biol Chem* 275: 1887–1896, 2000.
41. Thompson RJ, Zhou N, and MacVicar BA. Ischemia opens neuronal gap junction hemichannels. *Science* 312: 924–927, 2006.
42. Upham BL, Kang KS, Cho HY, and Trosko JE. Hydrogen peroxide inhibits gap junctional intercellular communication in glutathione sufficient but not glutathione deficient cells. *Carcinogenesis* 18: 37–42, 1997.
43. Valiunas V and Weingart R. Electrical properties of gap junction hemichannels identified in transfected HeLa cells. *Pflugers Arch* 440: 366–379, 2000.
44. Wang M, Martinez AD, Berthoud VM, Seul KH, Gemel J, Valiunas V, Kumari S, Brink PR, and Beyer EC. Connexin43 with a cytoplasmic loop deletion inhibits the function of several connexins. *Biochem Biophys Res Commun* 333: 1185–1193, 2005.
45. Yao J, Huang T, Fang X, Chi Y, Zhu Y, Wan Y, Matsue H, and Kitamura M. Disruption of gap junctions attenuates aminoglycoside-elicited renal tubular cell injury. *Br J Pharmacol* 160: 2055–2068, 2010.
46. Yao J, Oite T, and Kitamura M. Gap junctional intercellular communication in the juxtaglomerular apparatus. *Am J Physiol Renal Physiol* 296: F939–946, 2009.
47. Yao J, Suwa M, Li B, Kawamura K, Morioka T, and Oite T. ATP-dependent mechanism for coordination of intercellular $Ca^{2+}$ signaling and renin secretion in rat juxtaglomerular cells. *Circ Res* 93: 338–345, 2003.
48. Yao J, Zhu Y, Morioka T, Oite T, and Kitamura M. Pathophysiological roles of gap junction in glomerular mesangial cells. *J Membr Biol* 217: 123–130, 2007.
49. Yao J, Zhu Y, Sun W, Sawada N, Hiramatsu N, Takeda M, and Kitamura M. Irsogladine maleate potentiates the effects of nitric oxide on activation of cAMP signalling pathways and suppression of mesangial cell mitogenesis. *Br J Pharmacol* 151: 457–466, 2007.
50. Ye ZC, Wyeth MS, Baltan–Tekkok S, and Ransom BR. Functional hemichannels in astrocytes: A novel mechanism of glutamate release. *J Neurosci* 23: 3588–3596, 2003.
51. Yokouchi M, Hiramatsu N, Hayakawa K, Kasai A, Takano Y, Yao J, and Kitamura M. Atypical, bidirectional regulation of cadmium-induced apoptosis via distinct signaling of unfolded protein response. *Cell Death Differ* 14: 1467–1474, 2007.

52. Yokouchi M, Hiramatsu N, Hayakawa K, Okamura M, Du S, Kasai A, Takano Y, Shitamura A, Shimada T, Yao J, and Kitamura M. Involvement of selective reactive oxygen species upstream of proapoptotic branches of unfolded protein response. *J Biol Chem* 283: 4252–4260, 2008.
53. Zhao HB, Yu N, and Fleming CR. Gap junctional hemichannel-mediated ATP release and hearing controls in the inner ear. *Proc Natl Acad Sci USA* 102: 18724–18729, 2005.

Address correspondence to:
*Dr. Jian Yao*
*Department of Molecular Signaling*
*Interdisciplinary Graduate School of Medicine and Engineering*
*University of Yamanashi*
*Chuo, Yamanashi 409-3898*
*Japan*

*E-mail:* yao@yamanashi.ac.jp

Date of first submission to ARS Central, February 10, 2010; date of final revised submission, January 5, 2011; date of acceptance, January 14, 2011.

**Abbreviations Used**

BSO = DL-buthionine-[S,R]-sulfoximine
$Cd^{2+}$ = cadmium ions
$CdCl_2$ = cadmium chloride
Cx = connexin
Cx43 = connexin43
Cx43-MU = mutant connexin43
Cx54-WT = wild-type connexin43
DCF-DA = 2′, 7′-dichlorofluorescin diacetate
GJIC = gap junctional intercellular communication
GSH = glutathione
GSHee = glutathione reduced ethyl ester
JNK = c-Jun N-terminal kinase
LDH = lactate dehydrogenase
LY = Lucifer Yellow
NAC = N-acetyl-cysteine
PI = propidium iodide
ROS = reactive oxygen species

**This article has been cited by:**


1. Daniel Chevallier, Diane Carette, Dominique Segretain, Jérome Gilleron, Georges Pointis. 2012. Connexin 43 a check-point component of cell proliferation implicated in a wide range of human testis diseases. *Cellular and Molecular Life Sciences* . [CrossRef]
2. Claude Colomer, Agnès O. Martin, Michel G. Desarménien, Nathalie C. Guérineau. 2012. Gap junction-mediated intercellular communication in the adrenal medulla: An additional ingredient of stimulus–secretion coupling regulation. *Biochimica et Biophysica Acta (BBA) - Biomembranes* **1818**:8, 1937-1951. [CrossRef]
3. Kai Li, Jian Yao, Norifumi Sawada, Masanori Kitamura, Karl-Erik Andersson, Masayuki Takeda. 2012. #-Catenin Signaling Contributes to Platelet Derived Growth Factor Elicited Bladder Smooth Muscle Cell Contraction Through Up-Regulation of Cx43 Expression. *The Journal of Urology* **188**:1, 307-315. [CrossRef]
4. Qiaojing Yan, Kun Gao, Yuan Chi, Kai Li, Ying Zhu, Yigang Wan, Wei Sun, Hiroyuki Matsue, Masanori Kitamura, Jian Yao. 2012. NADPH oxidase-mediated upregulation of connexin43 contributes to podocyte injury. *Free Radical Biology and Medicine* . [CrossRef]